sustainability

MDPI

Article

Water Dynamics and Hydraulic Functions in Sandy Soils: Limitations to Sugarcane Cultivation in Southern Brazil

Jessica Lima Viana [1,*], Jorge Luiz Moretti de Souza [2], André Carlos Auler [2], Ricardo Augusto de Oliveira [3], Renã Moreira Araújo [3], Aaron Kinyu Hoshide [1,4], Daniel Carneiro de Abreu [1,5] and Wininton Mendes da Silva [6]

1 AgriSciences, Universidade Federal de Mato Grosso, Caixa Postal 729, Sinop 78550-970, MT, Brazil
2 Departamento de Solos e Engenharia Agrícola (DSEA), Universidade Federal do Paraná, Campus Universitário de Curitiba, Rua dos Funcionários 1540, Curitiba 80035-050, PR, Brazil
3 Departamento de Fitotecnia e Fitossanitarismo (DFF), Universidade Federal do Paraná, Campus Universitário de Curitiba, Rua dos Funcionários 1540, Curitiba 80035-050, PR, Brazil
4 College of Natural Sciences, Forestry and Agriculture, The University of Maine, Orono, ME 04469, USA
5 Instituto de Ciências Agrárias e Ambientais (ICAA), Universidade Federal de Mato Grosso, Campus Universitário de Sinop, Avenida Alexandre Ferronato 1200, Sinop 78550-728, MT, Brazil
6 Empresa Mato-Grossense de Pesquisa, Assistência e Extensão Rural (EMPAER-MT), Centro Político Administrativo, Cuiabá 78049-903, MT, Brazil
* Correspondence: jessica.limavp@gmail.com; Tel.: +55-66-9966-6763

Abstract: Crop cultivation on sandy soils is susceptible to water stress. Therefore, we determined the physical-hydric attributes of a Latossolo Vermelho distrófico (Oxisol) in northwestern Paraná state, Brazil. Soil samples were collected at depth ranges of 0 to 0.2 m, 0.2 to 0.4 m, and 0.4 to 0.6 m. We measured clay, silt, sand, fine and coarse sand contents, soil particle density, soil bulk density, total porosity, microporosity, and macroporosity. We also measured soil characteristics such as saturated and unsaturated soil hydraulic conductivities, pore distribution, water retention, available water capacity, and easily available water. We also estimated soil moisture, matric potential at field capacity, and time at field capacity. Validation of associations among these soil physical-hydric attributes was performed using principal component analysis. For the sandy soils analyzed, the distributions of coarse and fine sand fractions were measured for better evaluation of the soil's physical and hydric attributes. Higher coarse sand contents increased soil hydraulic conductivities, maximum pore diameter, and macroporosity while reducing microporosity. Fine sand content reduced conductivity and increased soil water retention in subsurface layers. Simulated sugarcane yield increased with soil water storage. These results support improving crop simulation modeling of sugarcane to support sustainable intensification in regions with sandy soils.

Keywords: available water capacity; hydraulic conductivity; pore distribution curve; retention curve; soil texture

Citation: Viana, J.L.; de Souza, J.L.M.; Auler, A.C.; de Oliveira, R.A.; Araújo, R.M.; Hoshide, A.K.; de Abreu, D.C.; da Silva, W.M. Water Dynamics and Hydraulic Functions in Sandy Soils: Limitations to Sugarcane Cultivation in Southern Brazil. *Sustainability* **2023**, *15*, 7456. https://doi.org/10.3390/su15097456

Academic Editor: Jan Hopmans

Received: 31 January 2023
Revised: 22 April 2023
Accepted: 25 April 2023
Published: 1 May 2023

1. Introduction

Physical-hydric attributes are used to understand and evaluate soil variability and quality, aeration, hydraulic conductivity, water redistribution, storage capacity, water availability to plants, and root growth [1–3]. Soil density, texture, total porosity, and saturated soil hydraulic conductivity are physical-hydric attributes used as primary indicators to monitor soil quality [4]. Sandy soils are associated with high hydraulic conductivity, and higher proportions of the coarse sand fraction are associated with reduced water availability [5,6].

In addition to intrinsic factors, soil use and management interfere with soil water retention [7] and consequently water availability for plants. A previous study on soil developed from sandstone in the 0 to 0.4 m layer, found 48.6 mm and 58.7 mm of available water capacity (AWC) in soil under crop-livestock integration and pineapple, respectively [6].

This difference of 10.1 mm was influenced by land use and management. Due to the intense management of the sugarcane crop, knowledge of the physical-hydric attributes of the soil is important, especially for crops established on sandy soils. The effect of sugarcane cultivation can increase soil bulk density, reaching critical values of 1760 and 1770 kg/m^3 in layers 0 to 0.2 m and 0.2 to 0.4 m, respectively, in medium texture Oxisol [8].

In sandy soils, there are differences in soil water retention due to the particle size composition of the sand fraction [9]. High proportions of medium and fine sand in sandy soils favor the formation of a capillary distribution network with smaller diameter pores, allowing water retention between soil particles. This matrix provides less soil moisture loss from percolation and, consequently, greater water storage due to the high percentages of finer particles (between 40% and 75% of total sand), combined with low clay content (i.e., particle diameters < 0.02 mm). Although typically less of a contributing factor, clay content can also contribute to increased water retention in sandy soils [9].

The Experimental Station of the Sugarcane Genetic Improvement at the Federal University of Paraná, in collaboration with the Inter-University Network for the Development of Sugarcane Energy, annually conducts numerous studies aimed at genetic improvement and productivity of sugarcane [10,11]. The results obtained in the experiments developed at this Experimental Station are a reference for numerous agricultural planning activities in the northwest region of Paraná state in southern Brazil. However, no detailed study of the physical-hydric attributes has yet been conducted for soils on the Experimental Station that represent a large number of Oxisols in the region. Obtaining information about the dynamics of water in the soil, especially because it is a region dominated by soils developed in the Caiuá Sandstone, may help in decision making regarding the selection of sugarcane varieties better adapted to water stress conditions. The survey of physical and hydric attributes can also subsidize water management in irrigated areas in sandy soils in northwestern Paraná. In this context, the goals and objectives of our research were to (1) determine the main physical-hydric attributes of the Latossolo Vermelho distrófico (Oxisol) cultivated with sugarcane in the northwestern region of Paraná state in Brazil, and (2) evaluate this soil's physical qualities for supporting the sugarcane crop.

2. Materials and Methods

2.1. Study Site Characteristics

This work was developed in the Laboratory of Modeling of Agricultural Systems (LAMOSA) at the Setor de Ciências Agrárias (SCA) at the Federal University of Paraná (UFPR). The analyses were performed using soil samples taken from the Experimental Station of the Sugarcane Genetic Improvement Program (PMGCA), belonging to UFPR and to the Inter-University Network for the Development of Sugarcane Energy (RIDESA). The soil of the Paranavaí Experiment Station is classified as Latossolo Vermelho distrófico (Oxisol) [12]. The PMGCA is located at 22°58′ South latitude, 52°28′ West longitude and is at 470 m of average altitude in the municipality of Paranavaí, located in the northwestern region of the Paraná state, Brazil. The climate of the region, according to the Köppen classification is Cfa (subtropical climate) and has an average annual air temperature between 22.1 and 23 °C, with average annual precipitation between 1400 and 1600 mm [13].

The geomorphology of northwestern Paraná is characterized by the Caiuá sandstone, with an area of 3.2 million hectares, representing 16% of the state area [14]. The Caiuá formation consists of deposits of eolic and fluvial environments, represented by fine to medium sandstones that are purplish with large cross-stratification [15]. According to Costa et al., 2020, the low natural fertility is due to the high sand content associated with the predominance of minerals of low activity in the clay fraction [16]. Latossolo soils associated with the Caiuá sandstone can also be highly susceptible to erosion as well as vertical subsurface soil water movement [17]. According to Pereira 2016, the Caiuá Aquifer is an important water source for the northwest region of the state of Paraná, with an outcrop area of approximately 30,000 km^2. This aquifer is characterized by being free and porous, with bicarbonated calcic to calcium-magnesian waters. The aquifer is composed of aeolian

sandstones from the Caiuá Group, which were deposited during the Upper Cretaceous over a paleo-depression formed by the basaltic flows of the Serra Geral Formation [18].

2.2. Soil Attributes

In order to determine soil physical-hydric attributes, we collected soil samples at ten representative points in the experimental area during July 2019. Interval soil sampling was conducted for the soil layers at depths of 0 to 0.2, 0.2 to 0.4, and 0.4 to 0.6 m. Soil analyses were performed using the Soil Physics Laboratories of the Soil and Agricultural Engineering Department at UFPR and in the Rural Development Institute (IDR) in Londrina, Paraná state in Brazil.

The deformed samples were collected with a flat bottom scoop, dried in an oven at 40 °C, sieved through a 2 mm mesh, and stored in plastic bags. After that, the clay, silt, and sand contents were gravimetrically determined using the pipette method [19]. Separation of the total sand fraction into coarse sand (0.2 to 2 mm) and fine sand (0.05 to 0.2 mm) was also performed. These grain fractions were then weighed (g/kg), according to the methodology developed by Embrapa [19]. Soil particle density (ρ_P; kg/m^3) was determined by the modified volumetric balloon method [20] using the formula:

$$\rho_P = \frac{M_{vs} - M_v}{50 - \left(\frac{M_{vsa} - M_{vs}}{\rho_a}\right)} \quad (1)$$

where ρ_P is the particle density of soil (kg/m^3), M_{vs} is the mass of the volumetric flask containing soil (kg), M_v is the mass of the volumetric flask (kg), M_{vsa} is the mass of the volumetric flask containing soil plus alcohol (kg), ρ_a is the density of the alcohol (kg/m^3), determined by the relationship between M_a and V_v, where M_a is the mass of alcohol (kg), and V_v is the volume of the flask (m^3).

2.3. Saturated Soil Hydraulic Conductivity

The un-deformed soil samples were collected in duplicate at each sampling point with the aid of volumetric rings (4.69 cm internal diameter and 3.51 cm height) and an Uhland sampler. After adequate preparation, the samples were saturated using capillary rise. After saturation, the saturated soil hydraulic conductivity (K_S measured as cm/hour) was determined by the Constant Load Permeameter method [21]:

$$K_S = \frac{V \cdot H}{(H + h) \cdot A \cdot t} \quad (2)$$

where K_S is the saturated hydraulic conductivity (cm/hour), V is the volume of percolated water (cm^3), H is the height of the cylindrical ring with soil (cm), h is the water sheet over the sample (cm), A is the cross-sectional area of the sample (cm^2), and t is the percolation time (hours).

Total porosity (TP), measured in cubic meters (m^3) of air space per volume of soil (m^3), was considered equal to the volumetric soil moisture at saturation (θs), which was also measured in m^3/m^3 of soil. The microporosity measured in m^3/m^3 of soil corresponded to the volumetric moisture of the soil sample submitted to a tension of −6 kilopascals (kPa). The macroporosity also measured in m^3/m^3 of soil was obtained by taking the difference between the value for TP and the value for microporosity [19].

2.4. Soil Water Retention

The soil samples were submitted to tensions of −6 and −10 kPa in a tension table and −33, −100, −500, and −1500 kPa in a Richards chamber. After each applied matric potential, the samples were dried at 105°C for 48 h for the determination of soil bulk density and volumetric moisture (θ), according to the methodologies developed at Embrapa [19]. The "θ vs. ψ_m" points and the moisture at saturation were used to determine the soil water retention curve (SWRC), fitted with the model of van Genuchten 1980 [22] using the Burdine

1953 restriction [23]. The adjustment of the parameters of the van Genuchten model and estimation of the volumetric soil moisture ($\hat{\theta}$) was performed with the *nls* function of the open-course statistical software program R version 4.0.0 [24]:

$$\Theta = \frac{\theta(\psi_m) - \theta r}{\theta s - \theta r} = \frac{1}{\left[1 + |\alpha \cdot \psi_m|^n\right]^m} \quad (3)$$

where Θ is the effective saturation (dimensionless), $\theta(\psi_m)$ is the volumetric soil moisture (m^3/m^3), θr is the residual volumetric soil moisture (m^3/m^3), θs is the volumetric soil moisture at saturation (m^3/m^3), ψ_m is the matric potential of water in the soil (kPa), α the value of air input per kPa, n is the empirical parameter of the fit (dimensionless), and m the Burdine restriction where $m = 1 - (2/n)$. The volumetric soil moisture (θ_{hco}) measured in m^3/m^3 at the pore water suction point in the hydraulic cut-off (ψ_{hco} measured in kPa) was calculated according to Czyz and Dexter 2013 [25] considering $\psi_{hco} = -1030$ kPa.

2.5. Unsaturated Soil Hydraulic Conductivity and Soil Water Redistribution

The unsaturated soil hydraulic conductivity ($K(\theta)$), measured in cm/hour, was calculated using the van Genuchten–Burdine equation:

$$K(\theta) = K_S \cdot \Theta^2 \cdot \left[1 - \left(1 - \Theta^{\frac{1}{m}}\right)^m\right] \quad (4)$$

The volumetric soil moisture (θ) at potentials -1 to -6 kPa was calculated (for matric potential or ψ less than -6 kPa the water is retained) to estimate $K(\theta)$. Subsequently, the $K(\psi)$ plot was prepared for soil layers at 0 to 0.2 m, 0.2 to 0.4 m, and 0.4 to 0.6 m depths.

In order to estimate the effective saturation (Θ), which was calculated using the actual volumetric moisture at field capacity ($\hat{\theta}_{CC}$):

$$\Theta = \frac{\hat{\theta}_{CC} - \theta r}{\theta s - \theta r} = \frac{1}{(1 + |\alpha \cdot \psi_{CC}|^n)^m} \quad (5)$$

and in order to estimate the matric potential at field capacity (ψ_{CC}):

$$\psi_{CC} = \frac{\left[\left(\frac{\theta s - \theta r}{\hat{\theta}_{CC} - \theta r}\right)^{\frac{1}{m}} - 1\right]^{\frac{1}{n}}}{\alpha} \quad (6)$$

It was assumed that this condition was reached when the drainage rate (τ) was defined as a percentage (p) of the saturated hydraulic conductivity (K_S) based on Prevedello 1999 [26] as restricted by Burdine 1953 [23]. The equations involving this assumption are as follows:

$$\tau = K(\theta) \quad (7)$$

$$\tau = K_S \cdot \Theta^2 \cdot \left[1 - \left(1 - \Theta^{\frac{1}{m}}\right)^m\right] \quad (8)$$

$$p = \frac{\tau}{K_S} = \Theta^2 \cdot \left[1 - \left(1 - \Theta^{\frac{1}{m}}\right)^m\right] \quad (9)$$

Based on Sisson et al., 1980 (Equation (10)) [27] and Prevedello and Armindo 2015 (Equation (11)) [28], an analytical model of soil water redistribution was obtained. For this, Equation (4) was derived with respect to θ and equalized to z/t:

$$\frac{z}{t} = \frac{dK}{d\theta} \quad (10)$$

$$\frac{dK}{d\theta} = \frac{dK}{d\Theta} \cdot \frac{d\Theta}{d\theta} \quad (11)$$

Then, the time corresponding to the field capacity in each soil layer was obtained:

$$\frac{z}{t_{CC}} = \left[\left(K_S \cdot (2 \cdot \Theta) \cdot \left(1 - \left(1 - (\Theta)^{\frac{1}{m}}\right)^{m}\right) + K_S \cdot (\Theta)^2 \cdot \left(\left(1 - (\Theta)^{\frac{1}{m}}\right)^{m-1} \cdot \left(m \cdot \left((\Theta)^{\frac{1}{m}-1} \cdot \frac{1}{m}\right)\right)\right)\right) \cdot \left(\frac{1}{(\theta s - \theta r)}\right)\right] \quad (12)$$

where p is the percentage of K_S (where we considered the values: 0.005; 0.010; 0.015; 0.020; 0.025; 0.030; 0.040; and 0.050), Θ is the effective saturation (dimensionless), m is the parameter from the Burdine (1953) restriction (dimensionless) [23]; t_{CC} is the time corresponding to the field capacity (h), z is the soil layer (m), and K_S is the saturated hydraulic conductivity (m/h). Estimation of the Θ function was performed in a routine developed in the R statistical program [24]. The moisture at the inflection point ($\hat{\theta}_{IP}$ measured in m^3/m^3) of the soil water retention curve was determined according to Dexter and Bird (2001) [29], and the respective matric potential at the inflection point (ψ_{IP} measured in kPa) was estimated using Equation (9) as:

$$\hat{\theta}_{IP} = (\theta s - \theta r) \cdot \left(1 + \frac{1}{m}\right)^{-m} + \theta r \quad (13)$$

2.6. Soil Water Capacity Function

The soil pore size distribution, represented by the water capacity function, was estimated using the retention curve model and capillarity theory [3,30]. The van Genuchten (1980) model was modified by replacing the matric potential ψ_m with the pore radius (r), using the capillarity equation [3]:

$$\theta = \theta r + \frac{(\theta s - \theta r)}{\left[1 + \left(\frac{A}{r}\right)^{n}\right]^{m}} \quad (14)$$

$$A = 2 \cdot \sigma \cdot \alpha \cdot 10^3 \quad (15)$$

With the derivative of the modified model, one obtains the following expressions for r_{max} (maximum pore radius) and d_{max} (maximum pore diameter):

$$\frac{d\theta}{d\log r} = (\theta s - \theta r) \cdot m \cdot n \cdot A^n \cdot r^{-n} \cdot (1 + A^n \cdot r^{-n})^{-m-1} \quad (16)$$

Deriving and equating to zero, one has:

$$r_{max} = A \cdot \left(\frac{1}{m}\right)^{-\frac{1}{n}} \quad (17)$$

$$d_{max} = 2 \cdot r_{max} \quad (18)$$

where σ is the surface tension of water (N m^{-1}); r is the pore radius measured in micrometers (μm).

2.7. Theoretical and Actual Soil Water Storage and Availability

The available soil water capacity (AWC) was determined from soil moisture measured at −6 kPa (AWC_1) and estimated from matric potential at field capacity (AWC_2), relative to the −1500 kPa matric potential:

$$AWC_1 = \sum_{i=1}^{n} (\theta_{CCi} - \theta_{PMPi}) \cdot z_i \quad (19)$$

$$AWC_2 = \sum_{i=1}^{n} (\hat{\theta}_{CCi} - \theta_{PMPi}) \cdot z_i \quad (20)$$

where AWC is measured in millimeters; θ_{CCi} the volumetric soil moisture at field capacity in the *i*th layer (m^3/m^3) at the matric potential of −6 kPa; θ_{PMPi} the volumetric soil moisture at the permanent wilting point in the *i*th layer (m^3/m^3) at the matric potential of −1500 kPa, $\hat{\theta}_{CC}$ the estimated soil volumetric moisture at field capacity in the *i*th layer (m^3/m^3) at the matric potential ψ_{CC}; z_i is the thickness of the *i*th soil layer (mm); and n the number of layers considered, which is dimensionless.

Considering the results obtained from the soil water redistribution and point of hydraulic cut-off, the easily available water (EAW) at matric potential −6 kPa (EAW_1) and ψ_{CC} (EAW_2) was determined in relation to the volumetric moisture at 1030 kPa −1030 kPa (ψ_{hco}):

$$EAW_1 = \sum_{i=1}^{n} (\theta_{CCi} - \theta_{hco}) \cdot z_i \quad (21)$$

$$EAW_2 = \sum_{i=1}^{n} (\hat{\theta}_{CCi} - \theta_{hco}) \cdot z_i \quad (22)$$

where EAW in the soil is measured in mm, θ_{hco} is the volumetric soil moisture at the matric potential of −1030 kPa in the *i*th layer (m^3/m^3), z_i is the thickness of the *i*th soil layer (mm), and n is the number of layers considered and is dimensionless. Available soil water capacity (AWC) and easily available water (EAW) were calculated for different soil layers at four percentages of AWC and EAW: 100%, 80%, 60%, and 40%. These values were then summarized using R software's *ggplot2* function [24].

2.8. Statistical Analyses

Descriptive statistics were used to analyze our results with the help of the boxplot graph, and the discriminant values (outliers) were removed from the subsequent analyses with 6 repetitions. The assumptions of normality and homogeneity of variances were verified with the Shapiro–Wilk and Bartlett tests, respectively. Once these assumptions were met, the data were submitted for analysis of variance and the averages were compared using the Tukey test at the 5% significance level. The t_{CC} data were submitted to the Kruskal–Wallis test. Statistical errors and index between observed (Y) and estimated ($\hat{Y}$) values were quantified with the following expressions for root mean square error (RMSE), the root mean square error normalized by the mean (NRMSE), the ratio of RMSE to the standard deviation (RSR), and Willmott's agreement index (d) [31,32]:

$$RMSE = \sqrt{\frac{\sum_{i=1}^{n} (\hat{Y}_i - Y_i)^2}{n}} \quad (23)$$

$$NRMSE = \frac{\sqrt{\frac{\sum_{i=1}^{n} (\hat{Y}_i - Y_i)^2}{n}}}{\overline{Y}} \quad (24)$$

$$RSR = \frac{RMSE}{Dp_Y} \quad (25)$$

$$d = 1 - \left[\frac{\sum_{i=1}^{n} (\hat{Y}_i - Y_i)^2}{\sum_{i=1}^{n} (|\hat{Y}_i - \overline{Y}| + |Y_i - \overline{Y}|)^2} \right] \quad (26)$$

with measurement units specified for RMSE (m^3/m^3), NRMSE (%), RSR (dimensionless), and d (dimensionless). For RMSE, NRMSE, and d, $\hat{Y}_i$ is the *i*th value of the estimated variable (m^3/m^3), Y_i is the *i*th value of the observed variable (m^3/m^3), and n is the amount of data for the observed variable (units of variable). When calculating NRMSE and d, $\overline{Y}$ is the mean of the values of the observed variable (m^3/m^3). For RSR calculation, Dp_Y is the standard deviation of the observed data (m^3/m^3).

Validation of the associations among soil physical-hydric attributes was performed using principal component analysis (PCA). The correlation matrix of the standardized

variables (unit variances and zero means) of each soil layer was used in PCA. The *prcomp* function was used to perform PCA and the *ggfortify* package [33] of the R software [24] was used for graphing.

2.9. Sugarcane Yield Modeling

The 12 years at the research site where sugarcane cultivars were evaluated were 1998–2006, 2008, and 2018–2019. Over these years, there were four sugarcane cultivars that were tested. RB72454 was planted from 1998 to 2006 and in 2008. RB867515 was trialed from 2004 to 2006 and from 2018 to 2019. RB966928 was evaluated from 2004 to 2005 and from 2018 to 2019. Finally, RB036066 was planted in 2018 and 2019. Sugarcane was grown in all years without irrigation.

Simulated sugarcane yields were estimated using soil water storage values (AWC and EAW, considered at 100%) from this study entered into a model validated from 12 years of field data from UFPR and RIDESA by Viana et al., 2023 [34]:

$$TCH = -986.016 - 0.288 \times ADD_I + 165.645 \times SWS_{II} \quad (27)$$

In the simulation, the logarithmic transformation of the multiple linear regression model was performed:

$$TCH = e^{-11.3374} \times ADD_I{}^{-0.8224} \times SWS_{II}{}^{10.5272} \quad (28)$$

where TCH is metric tons of sugarcane stalk per hectare, ADD_I is growing degree days (°C) during the first stage of sugarcane crop development (July through October), and SWS_{II} is soil water storage during the second development (October through March) for a 12-month production period. The third stage of development runs from March through July where the crop accumulates sucrose [34]. Simulated yields (*y*-axis) were then graphed three-dimensionally against SWS_{II} (AWC and EAW) measured in cm (*x*-axis) and ADD_I measured in °C (*z*-axis) for all data points. Graphing was performed using R's *scatter3d plotly r* function [24].

3. Results

3.1. Texture and Sandy Soil Structure

Clay content was significantly higher in the 0.2 to 0.4 and 0.4 to 0.6 m layers of soil compared to the topsoil layer at 0 to 0.2 m depth (Table 1). There was an inverse relationship between coarse and fine sand fractions in the soil profile (Table 1). The soil bulk density (ρ_S) and particle density (ρ_P) did not show significant differences among the soil layers (Table 1). The magnitude of the values we found is consistent with what is expected from sandy texture soils [1]. The soil bulk densities we measured (Table 1) ranged from 1582 to 1690 kg/m^3 which were consistent with an expected range of 1300 to 1800 kg/m^3 [30]. The average value of total porosity (TP = 0.33 m^3/m^3) was low, as commonly observed in sandy soils with fine sand contents [2,35]. As macroporosity decreased, microporosity increased, but ρ_S did not increase and TP decreased ($p < 0.05$) in the subsurface layers (Table 1). There was an increase in microporosity and clay contents at depth.

Table 1. Physical-hydric attributes of *Latossolo Vermelho distrófico* (Oxisol) soil layers at the Sugarcane Genetic Improvement Program Experimental Station cultivated with sugarcane in Paranavaí, Paraná state, Brazil.

Soil Layer	Sand Classification [1]			Silt	Clay	Soil Density [1]		Soil Porosity [1]		
	Total	Coarse	Fine			Particle	Bulk	Total	Macro	Micro
m		g/kg				kg/m^3		m^3/m^3		
0.00–0.20	838 a	770 a	121 b	67.6 a	94.8 b	2710 a	1580 a	0.331 a	0.158 a	0.173 b
0.20–0.40	793 b	685 b	135 b	64.3 b	143 a	2722 a	1690 a	0.316 a	0.0906 b	0.225 a
0.40–0.60	785 b	627 b	167 a	65.4 b	150 a	2703 a	1650 a	0.329 a	0.0883 b	0.241 a
Average	805	694	140	65.8	129	2712	1640	0.325	0.112	0.213
Var [2]	571	3620	402	1.99	633	2216.8	10,600	<0.001	0.00167	0.00107
Stdev [3]	23.9	60.2	20.1	1.41	25.2	47.08	103	0.0205	0.0409	0.0326
CV [4]	2.97%	8.67%	14.2%	2.15%	19.5%	1.74%	6.27%	6.31%	36.4%	15.3%

[1] Averages followed by equal letters in the column do not differ by the Tukey test at 5% probability. [2] Var is the variance (variable unit). [3] Stdev is the standard deviation (variable unit). [4] CV is the coefficient of variation (%).

3.2. Water Movement in Sandy Soil

The saturated hydraulic conductivity (K_S) was higher in the 0 to 0.2 m layer and reduced abruptly at depth (Figure 1a) due to macroporosity facilitating water drainage in saturated soil [35]. Like Ks, unsaturated hydraulic conductivity K(θ) was also higher in the uppermost soil layer. However, the decrease in K(θ) with the reduction in soil moisture was more significant in the 0 to 0.2 m layer, compared to the others (Figure 1b). The K(ψ) in the surface layer showed greater decay (Figure 1c) with increasing matric potential due to the smaller number of capillary pores [35].

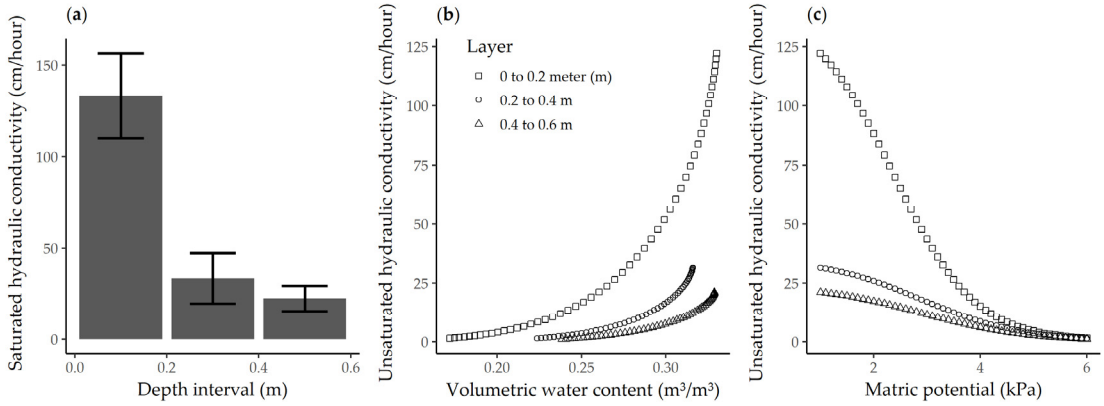

Figure 1. (**a**) Saturated (K_S) conductivity with error bars in cm/hour; (**b**) unsaturated (K(θ)) hydraulic conductivity versus volumetric water content; and (**c**) versus matric potential in the soil layers 0 to 0.20 m (m), 0.2 to 0.4 m, and 0.4 to 0.6 m for the Latossolo Vermelho distrófico (Oxisol) at the Sugarcane Genetic Improvement Program Experimental Station cultivated with sugarcane in Paranavaí, Paraná state, Brazil.

3.3. Water Retention and Pore Distribution

The soil water retention curves showed no evidence of compaction effects (Figure 2), as the soil bulk density (ρ_S) values are below the critical value of $\rho_S > 1.70$ g/cm^3 [2]. The parameters of the van Genuchten model (α and n) were significant ($p < 0.05$) to represent the soil water retention curve for all soil layers (Table 2). Statistical errors and indices between observed (θ) and estimated ($\hat{\theta}$) soil volumetric moisture indicated that fits with the van Genuchten–Burdine model were satisfactory for the analyzed layers (Table 3). Among the errors, the NRMSE was higher due to the use of the six repetitions at each matric potential to perform the adjustment of the soil water retention curve, which improved the significance of the adjustment.

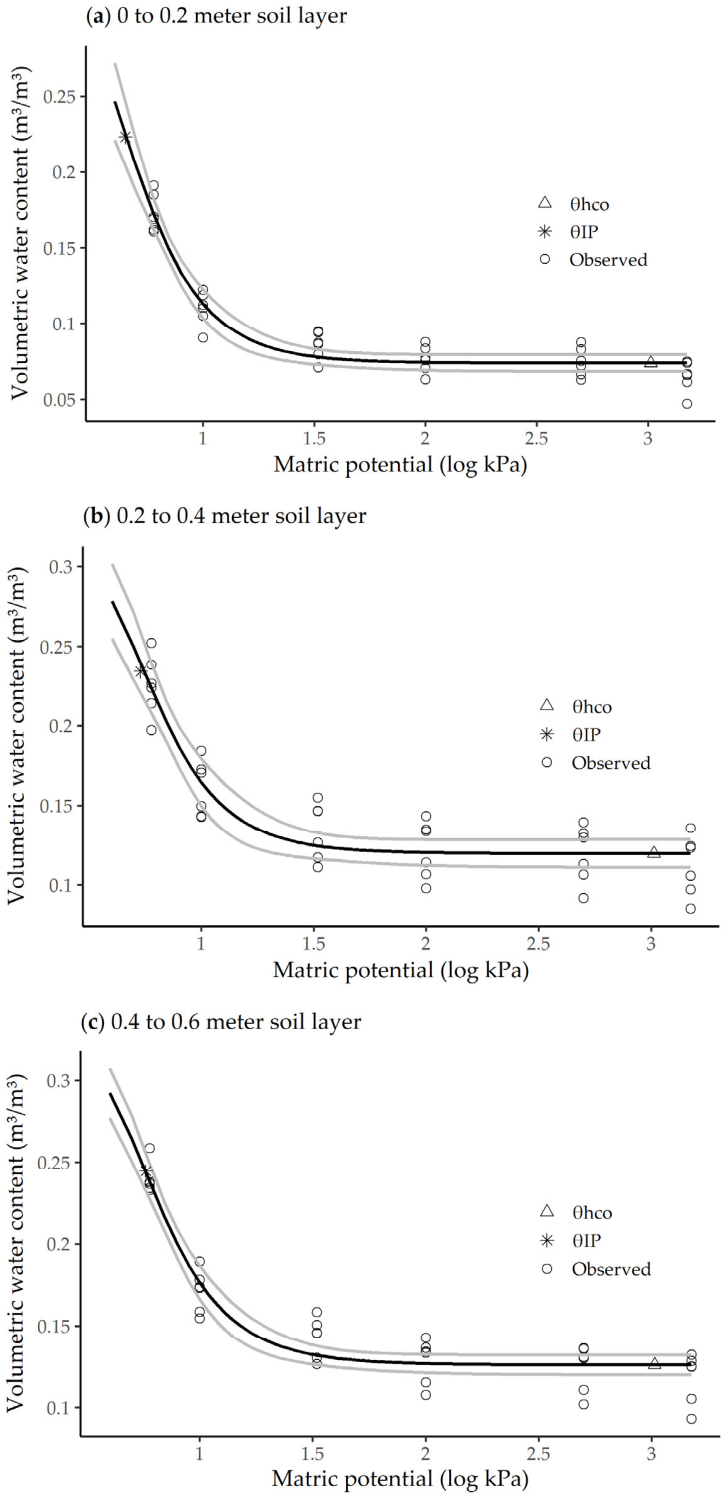

Figure 2. The water retention curve of the Latossolo Vermelho distrófico (Oxisol) in the layers (**a**) 0 to 0.2 m; (**b**) 0.2 to 0.4 m; and (**c**) 0.4 to 0.6 m. The fitted values are accompanied by the confidence band for the predicted value.

The RSR is one of the quantitative statistics recommended by Moriasi et al. (2007) [36] to evaluate models. The smallest magnitudes of RSR were observed at different p in the soil layers due to the physical-hydric attributes of the soil (Table 4). Lower matric potential ψ_{IP} was found in the 0 to 0.2 m (m) layer due to the soil texture (Table 5). The pore distribution curve (Figure 3) showed a maximum pore diameter (d_{max}) of 64.19 μm (μm) at a soil depth

of 0 to 0.2 m, 51.96 µm at 0.2 to 0.4 m, and 50.6 µm at 0.4 to 0.6 m. The maximum point of the pore diameter frequency curve dθ/dlog(r) corresponded to 0.192 at a depth of 0 to 0.2 m, 0.1458 at 0.2 to 0.4 m, and 0.1463 at 0.4 to 0.6 m in the analyzed soil layers.

Table 2. Fitted parameters for the van Genuchten model and their confidence intervals.

Soil Layer Depth (Meter)	Parameter [1]	Estimated Value	Error	t-Statistic	Significance (*p*-Value)	95% Confidence Interval ($CI_{95\%}$)	Goodness of Fit (R^2)
0 to 0.2	θs (m^3/m^3)	0.331	0.00517	63.9	<0.001	[0.321; 0.341]	0.982
	θr (m^3/m^3)	0.0737	0.00283	26.0	<0.001	[0.0681; 0.0792]	
	α (1/kPa)	0.265	0.0275	9.63	<0.001	[0.211; 0.318]	
	n (ad.)	3.92	0.331	11.8	<0.001	[3.27; 4.57]	
0.2 to 0.4	θs (m^3/m^3)	0.316	0.008	39.1	<0.001	[0.300; 0.332]	0.932
	θr (m^3/m^3)	0.120	0.004	26.8	<0.001	[0.111; 0.128]	
	α (1/kPa)	0.215	0.0282	7.6	<0.001	[0.159; 0.270]	
	n (ad.)	3.90	0.507	7.68	<0.001	[2.90; 4.89]	
0.4 to 0.6	θs (m^3/m^3)	0.329	0.00558	59.0	<0.001	[0.318; 0.340]	0.969
	θr (m^3/m^3)	0.126	0.00311	40.4	<0.001	[0.120; 0.132]	
	α (1/kPa)	0.211	0.0183	11.6	<0.001	[0.175; 0.247]	
	n (ad.)	3.82	0.318	12.0	<0.001	[3.20; 4.45]	

[1] θs and θr are the soil moisture at saturation and residual, respectively, while α and n are the parameters of the van Genuchten model.

Table 3. Errors and statistical index between observed (θ) and estimated ($\hat{\theta}$) soil volumetric moisture with van Genuchten model using Burdine restriction.

Soil Layer Depth	Root Mean Square Error (RMSE)	Normalized RMSE	RMSE/Stdev (RSR)	Willmott's Agreement Index (d)
(m)	(m^3/m^3)	(%)	(ad.)	(ad.)
0 to 0.2	0.0121	13.4	0.134	0.995
0.2 to 0.4	0.0188	25.8	0.258	0.982
0.4 to 0.6	0.0130	17.5	0.175	0.992

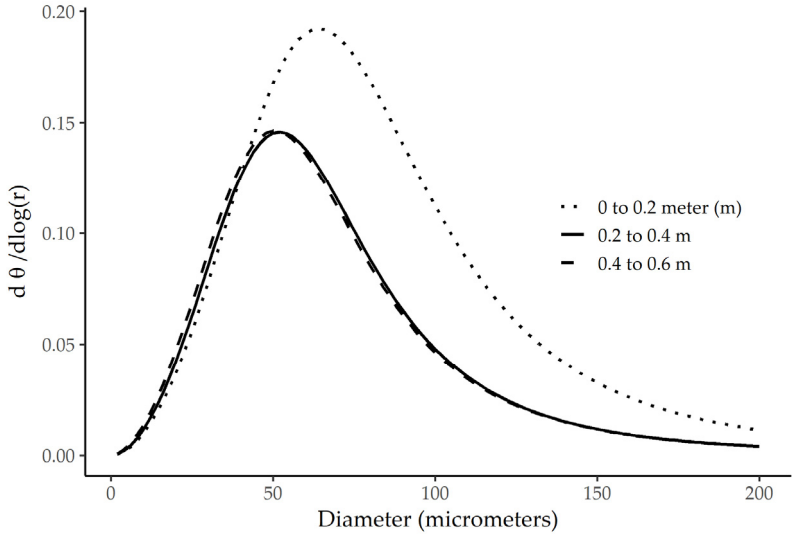

Figure 3. Pore distribution curve for soil layers at depths of 0 to 0.2 m, 0.2 to 0.4 m, and 0.4 to 0.6 m of Latossolo Vermelho distrófico (Oxisol) used for sugarcane cultivation at the Experimental Station of the Sugarcane Genetic Improvement Program at the Federal University of Paraná and the Inter-University Network for the Development of Sugarcane Energy.

Table 4. Estimated actual moisture ($\hat{\theta}_{CC}$), matric potential (ψ_{CC}), and time (t_{CC}) at field capacity and statistical error between observed (θ_{CC}) at –6 kPa and estimated ($\hat{\theta}_{CC}$) volumetric moisture at field capacity.

Soil Layer	**Percentage Ratio (p) of Saturated Hydraulic Conductivity (K_S)**							
Depth (m)	**0.005**	**0.010**	**0.015**	**0.020**	**0.025**	**0.030**	**0.040**	**0.050**
Estimated actual moisture at field capacity $\hat{\theta}_{CC}$ (m^3/m^3) [1]								
0 to 0.2	0.157 c	0.172 c	0.182 b	0.190 b	0.196 b	0.202 b	0.211 b	0.218 a
0.2 to 0.4	0.184 ab	0.195 ab	0.203 ab	0.209 ab	0.214 ab	0.218 ab	0.225 ab	0.230 a
0.4 to 0.6	0.192 a	0.204 a	0.212 a	0.218 a	0.223 a	0.228 a	0.235 a	0.240 a
Average	0.178	0.191	0.199	0.206	0.211	0.216	0.223	0.230
Var	0.000404	0.000366	0.000346	0.000332	0.000323	0.000315	0.000306	0.000300
Stdev	0.0201	0.0191	0.0186	0.0182	0.0180	0.0178	0.0175	0.0173
CV	11.3	10.1	9.34	8.87	8.51	8.24	7.83	7.54
Root mean square error/standard deviation (RSR) (dimensionless)								
0 to 0.2	1.96	1.57	1.78	2.15	2.52	2.87	3.49	4.02
0.2 to 0.4	2.41	1.88	1.57	1.37	1.23	1.15	1.10	1.15
0.4 to 0.6	5.20	4.00	3.23	2.66	2.23	1.89	1.47	1.35
Matric potential at field capacity (ψ_{CC} in kPa) [1]								
0 to 0.2	6.55 c	5.93 c	5.59 c	5.35 c	5.16 b	5.01 b	4.78 b	4.60 b
0.2 to 0.4	8.16 ab	7.38 ab	6.95 ab	6.64 ab	6.41 ab	6.23 ab	5.94 ab	5.71 ab
0.4 to 0.6	8.56 a	7.73 a	7.26 a	6.94 a	6.69 a	6.49 a	6.18 a	5.94 a
Average	7.76	7.01	6.60	6.31	6.09	5.91	5.63	5.42
Var	1.48	1.30	1.21	1.15	1.10	1.07	1.01	0.969
Stdev	1.22	1.14	1.10	1.07	1.05	1.03	1.01	0.985
CV	15.7	16.3	16.7	17.0	17.3	17.5	17.9	18.2
Time at field capacity (t_{CC} in hours) [1]								
0 to 0.2	0.604 c	0.355 c	0.259 c	0.207 c	0.174 c	0.151 c	0.120 c	0.101 c
0.2 to 0.4	1.85 b	1.08 b	0.791 b	0.633 b	0.532 b	0.461 b	0.367 b	0.307 b
0.4 to 0.6	2.84 a	1.67 a	1.22 a	0.975 a	0.819 a	0.710 a	0.566 a	0.473 a
Average	1.76	1.04	0.757	0.605	0.508	0.441	0.351	0.294
Var	0.953	0.328	0.175	0.112	0.079	0.060	0.038	0.027
Stdev	0.976	0.573	0.419	0.335	0.281	0.244	0.194	0.163
CV	55.3	55.3	55.3	55.3	55.4	55.4	55.4	55.4

[1] Averages followed by equal letters in the column do not differ by Tukey's test at 5% probability ($\hat{\theta}_{CC}$ and ψ_{CC}) and t_{CC} by Kruskal–Wallis test.

Table 5. Estimated moisture ($\hat{\theta}_{IP}$) and matric potential (ψ_{IP}) at the inflection point, and statistical error between observed (θ_{CC}) at –6 kPa and estimated ($\hat{\theta}_{IP}$) volumetric moisture at field capacity.

Soil Layer Depth (Meter)	**Estimated Moisture $\hat{\theta}_{IP}$ (m^3/m^3) [1]**	**Matric Potential ψ_{IP} (kPa) [1]**	**RSR (Dimensionless) [5]**
0 to 0.2	0.223 b	4.48 b	4.29
0.2 to 0.4	0.234 ab	5.37 ab	1.08
0.4 to 0.6	0.244 a	5.79 a	1.37
Average	0.234	5.21	-
Var [2]	0.000229	0.879	-
Stdev [3]	0.0151	0.938	-
CV [4]	6.48	18.0	-

[1] Averages followed by equal letters in the column do not differ by the Tukey test at 5% probability. [2] Var is the variance (variable unit). [3] Stdev is the standard deviation (variable unit). [4] CV is the coefficient of variation (%). [5] RSR—Root mean square error/Standard deviation (dimensionless).

3.4. Water Availability

In general, the soil of the experimental area cultivated with sugarcane showed low water availability for plants in the layers analyzed (Table 6), which is characteristic of soils with low clay contents [5,37]. There was no statistical difference between the layers

($p > 0.05$), but the highest AWC_1 and EAW_1 occur in the soil layers at 0.2 to 0.4 m and 0.4 to 0.6 m depth due to the higher amount of clay and microporosity [5]. The highest AWC_2 and EAW_2 occurred in the surface layer ($p < 0.05$) due to the higher organic carbon content that increases water retention and availability for plants [38]. This surface layer corresponds to the soil layer with the highest volume and density of root length for sugarcane [34]. Figure 4 shows the variation in the percentage of water availability for the soil in the experimental area at the Experimental Station of the Sugarcane Genetic Improvement Program at the Federal University of Paraná and the Inter-University Network for the Development of Sugarcane Energy.

Table 6. Hydric attributes of the *Latossolo Vermelho distrófico* (Oxisol), cultivated with sugarcane at the Experimental Station of the Sugarcane Genetic Improvement Program at the Federal University of Paraná and the Inter-University Network for the Development of Sugarcane Energy.

Soil Layer	θ_{CC} [1]	$\hat{\theta}_{CC}$ [1]	θ_{PMP} [1]	θ_{hco} [1]	AWC_1 [1]	AWC_2 [1]	EAW_1 [1]	EAW_2 [1]
Depth (m)	**m^3/m^3**				**mm**			
0.00–0.20	0.173 b	0.218 a	0.0650 b	0.0735 b	21.6 a	30.6 a	19.9 a	28.9 a
0.20–0.40	0.225 a	0.230 a	0.112 a	0.119 a	22.7 a	23.6 b	21.2 a	22.1 b
0.40–0.60	0.241 a	0.240 a	0.118 a	0.126 a	24.5 a	24.4 b	22.9 a	22.9 b
Average	0.213	0.229	0.0983	0.106	22.9	26.2	21.3	24.6
Var [2]	0.00107	0.000300	0.000804	0.000753	9.34	21.2	7.91	20.7
Stdev [3]	0.0326	0.0173	0.0283	0.0274	3.06	4.61	2.81	4.55
CV [4]	15.3	7.54	28.8	25.8	13.3	17.6	13.2	18.4

[1] Averages followed by equal letters in the column do not differ by the Tukey test at 5% probability. [2] Var is the variance (variable unit). [3] Stdev is the standard deviation (variable unit). [4] CV is the coefficient of variation (%).

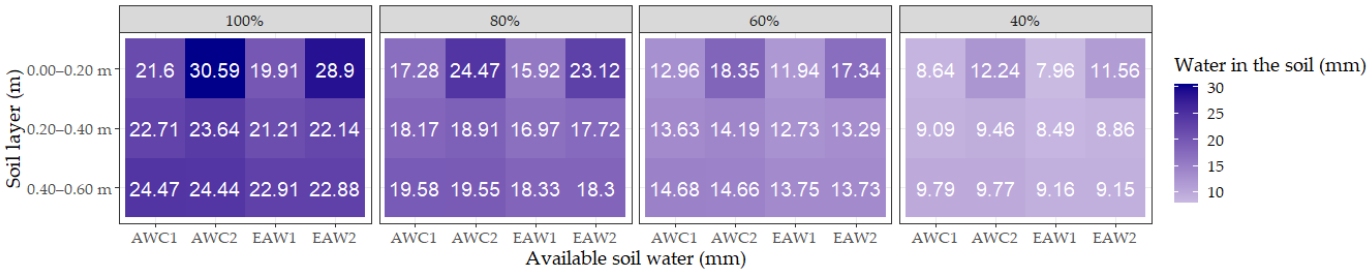

Figure 4. Water in the soil (mm) for different percentages of available soil water capacity (AWC_1 and AWC_2) and easily available water (EAW_1 and EAW_2) and for different soil layers (m).

3.5. Multivariate Relationships among Soil Physical-Hydric Attributes

Principal component analysis (PCA) was used to validate the previously established associations between the structural and hydric physical attributes. We observed that the first principal component (PC1) explained 60.6% of the total variance. PC1 (eigenvalue of 3.114) and PC2 (eigenvalue of 1.495) together explained 74.6% of the total variance (Figure 5).

PCA was efficient in distinguishing between soil layers. The 0 to 0.2 m layer was characterized and influenced mainly by the physical-hydric attributes of macroporosity, silt, saturated hydraulic conductivity, unsaturated hydraulic conductivity, sand, coarse sand, and maximum pore diameter. The variables fine sand, clay, microporosity, volumetric soil moisture at the permanent wilting point, volumetric soil moisture at the inflection point, soil density, and available soil water capacity determined at –6 kPa were higher and more expressive in the physical-hydric attributes of the soil layers at depths of 0.2 to 0.4 m and 0.4 to 0.6 m (Figure 5). It was found that saturated hydraulic conductivity showed a direct relationship with sand, coarse sand, silt, macroporosity, and maximum pore diameter, and inverse with microporosity, clay, volumetric soil moisture at the permanent wilting point, and fine sand. The soil density showed an inverse relationship with macroporosity.

Microporosity was directly related to clay, fine sand, and volumetric soil moisture at the permanent wilting point, and inversely with saturated hydraulic conductivity, sand, coarse sand, silt, macroporosity, and maximum pore diameter.

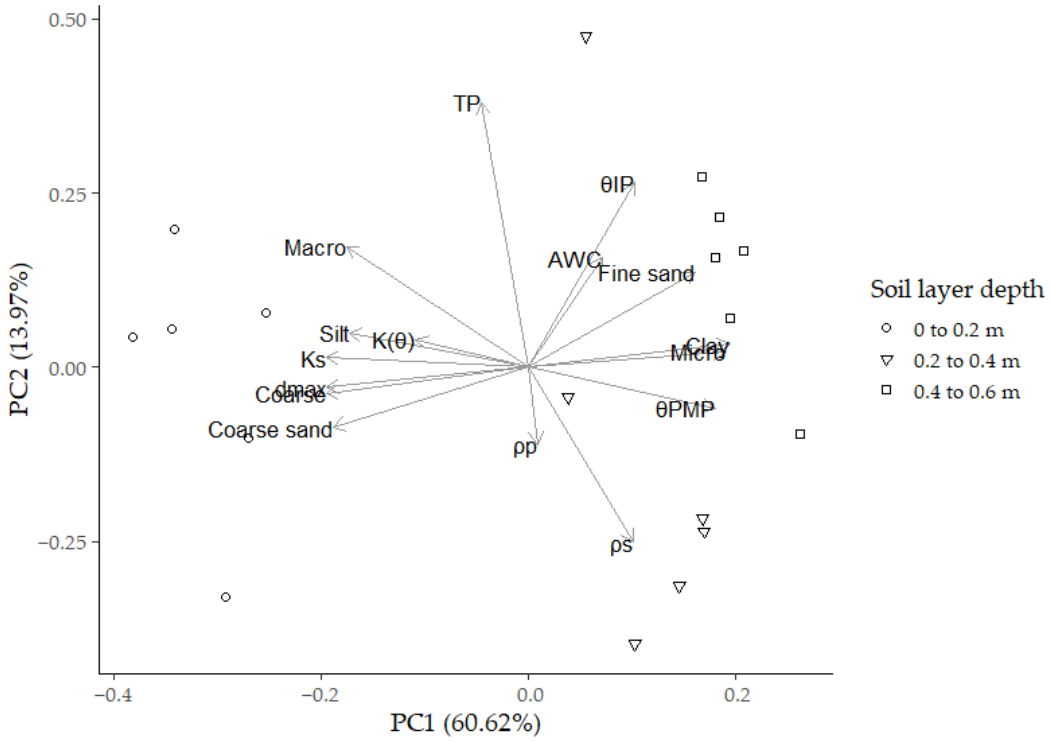

Figure 5. Principal component analysis (PCA) of the physical-hydric attributes of the Latossolo Vermelho distrófico (Oxisol), cultivated with sugarcane in the Experimental Station of the Sugarcane Genetic Improvement Program at the Federal University of Paraná and the Inter-University Network for the Development of Sugarcane Energy. Labels for (1) "dmax" and "Coarse" and (2) "Clay" and "Micro" slightly overlap with each other due to close proximity of these two pairs of vectors.

3.6. Sugarcane Yield Simulations

For 12 years at the research site, sugarcane stalk yield (TCH) averaged 114.68 metric tons (t)/hectare (ha). TCH was at a minimum of 65.997 t/ha in 2005 and a maximum of 164.190 t/ha in 2006 (Figure 6). Fracaro et al., 2014 [39] found sugarcane TCH of 170 t/ha for RB036152 and an average TCH of 110 t/ha across 26 genotypes from RIDESA in the 2013–2014 crop season in the municipality of Viamão, Rio Grande do Sul state, Brazil. The estimated Brazilian average national productivity of sugarcane for the 2022–2023 crop season, according to CONAB [40], is 72 t/ha. The 2022–2023 crop season was characterized by reduced rainfall and low temperatures in the Central-South Region, which accounts for around 90% of Brazil's total sugarcane production [40].

In the sugarcane model simulation with AWC and EAW set at a value of 100% (Figure 7), TCH for: (1) EAW_1 averaged 33.94 t/ha with a minimum of 26.84 t/ha and a maximum of 42.27 t/ha; (2) AWC_1 averaged 72.10 t/ha with a minimum of 57.00 t/ha and a maximum of 89.78 t/ha; (3) EAW_2 averaged 153.96 t/ha with a minimum of 121.73 t/ha and a maximum of 191.73 t/ha; and (4) AWC_2 averaged 296.58 t/ha with a minimum of 234.50 t/ha and a maximum of 369.34 t/ha. Under the 100% water availability condition in Phase II, EAW_1 underestimates and AWC_2 overestimates sugarcane yield. Analyzing the simulated values with EAW_2 (set at 100%), the potential yield of sugarcane can be achieved with sustainable management practices, genetic improvement, and favorable climate conditions.

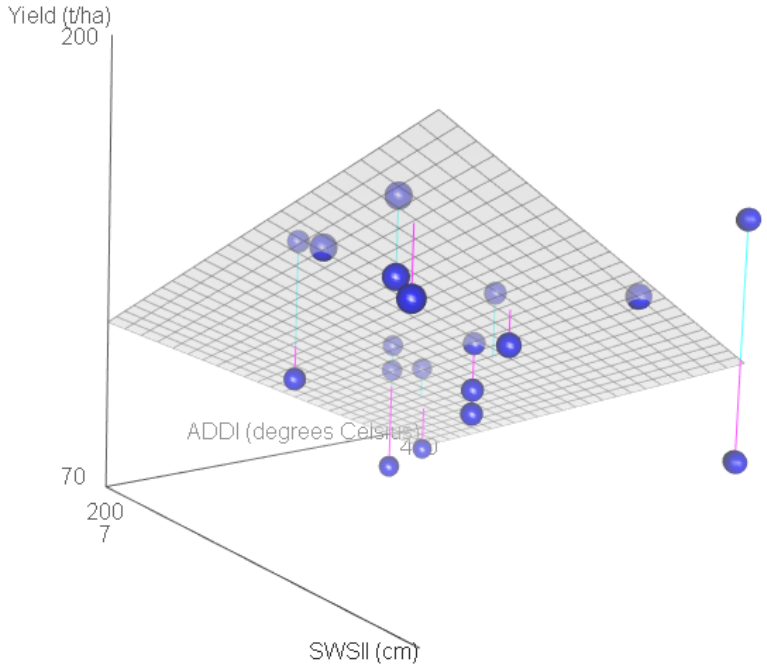

Figure 6. Sugarcane yield model validated from 12 years of field data from UFPR and RIDESA by Viana et al., 2023 [34].

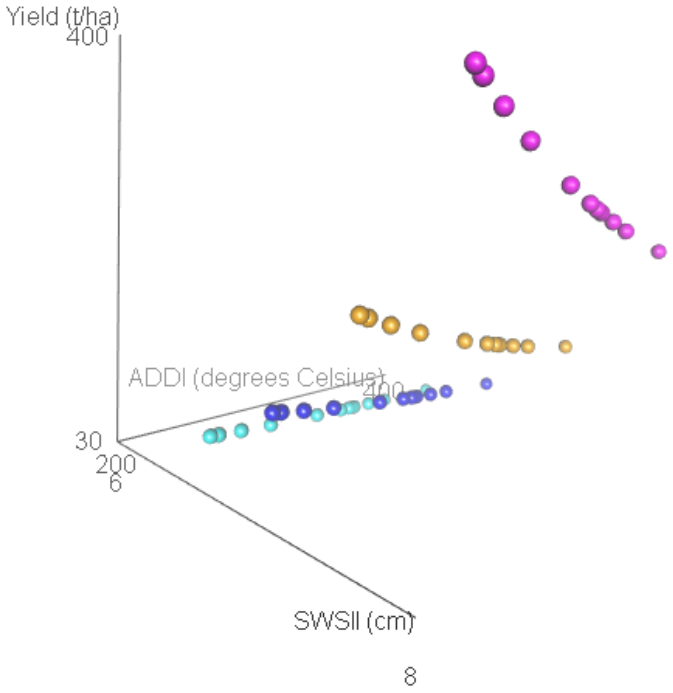

Figure 7. Simulated sugarcane stalk yield (TCH = t/ha) as a function of growing degree days during development phase I (ADD_I) and soil water storage during development phase II (SWS_{II}) using both AWC and EAW (100%), with the logarithmic transformation of the validated model by Viana et al., 2023 [34].

4. Discussion

4.1. Comparisons to Previous Research

4.1.1. Soil Characteristics

Although there was an increase in clay content in the subsurface layers, this did not result in abrupt textural changes in the soil. Greater clay content in lower soil surface layers

can result in increased water retention for sandy soils. As a consequence, the sand and silt contents were lower in the 0.2 to 0.4 m and 0.4 to 0.6 m soil layers. Thus, the analyzed soil is in the textural classes of sand in the soil layer at the depth range of 0 to 0.20 m, and loamy sand in soil layers 0.2 to 0.4 m and 0.4 to 0.6 m [41], characteristic of the Paranavaí Sandstone Formation in the northwestern region of Paraná [6]. The higher coarse sand content of the sand fraction is characteristic of soils of the Paranavaí region, confirmed by the granulometric characterization in areas of crop-livestock and pineapple integration in the Caiuá and Paranavaí Sandstone Formations [6]. Fidalski 2017 [42] considered that the granulometric characterization is a criterion to guide the use and management of soils of the Caiuá Sandstone in the northwestern region of Paraná. This is due to the inverse relationship of the sand contents (total or coarse) with the available water in the soil.

Souza et al., 2015 [37] found an average soil bulk density of 1620 kg/m^3 at the RIDESA. This was close to the average ρ_S obtained in this study of 1640 kg/m^3. In the literature, there are reports of root growth restriction in sugarcane for ρ_S = 1700 kg/m^3 [2]. Thus, the bulk density values obtained in this study between 1600 and 1700 kg/m^3 are at the threshold of possibly limiting crop root growth. Therefore, management practices should be adopted to minimize soil compaction.

Ortiz et al., 2017 [43] found TP between 0.29 and 0.38 m^3/m^3 in sandy soil grown in the first, third, and fifth sugarcane cycles in 44, 40, and 15 years of production, respectively. Low macroporosity pore values (0.09 m^3/m^3) were obtained in the soil layers at 0.2 to 0.4 m and 0.4 to 0.6 m (Table 1). This may be a problem since values lower than 0.1 m^3/m^3 are limiting to soil aeration and harmful to agricultural production [1,44,45]. These results support recommendations for better managing sandy soils, including reducing soil bulk density and increasing total porosity and macroporosity, especially in deeper soil layers [44].

4.1.2. Saturated Soil Hydraulic Conductivity

Our results indicate that the water dynamics in the soils that were analyzed can be modified between their layers since the microporosity is responsible for the retention and conduction of water in unsaturated soil, and macroporosity is responsible for the drainage and aeration of the soil [1,35]. High K_S values in more superficial layers are characteristic of sandy textured and well-drained soils [5]. However, especially in the 0.4 to 0.6 m layer, the abrupt change in K_S can make the soil susceptible to shear which may lead to erosion. The combination of high K_S and sand content account for more than 80% of the variability in soil loss [46]. Our results reinforce the need to increase macroporosity at depth to better manage sugarcane.

Even though the K_S in the surface layer was higher than the others (Figure 1a), the values were lower than in soils of other textures also cultivated with sugarcane [47,48]. Due to the effects of soil preparation recently performed for sugarcane re-planting such as chiseling and disking, Cherubin et al., 2016 [47] found K_S (measured in the field) of 250 cm/h in soil with medium clay texture, in the surface layer. The authors found that K_S showed a direct correlation with total porosity and macroporosity, and an inverse relationship with ρ_S and the degree of soil compaction, both of which may be directly influenced by soil management. Silva et al., 2018 [48] observed in sandy soils that K_S decreased with increasing depth in sandy soils, associated with increasing bulk density and microporosity. Silva et al., 2018 [48] found a direct correlation between K_S with coarse sand and medium sand fractions and an inverse correlation with the available water capacity. In addition, it was found that the available water capacity showed an inverse linear correlation with the coarse sand and medium sand grain size fractions, and direct linear correlation with the micropore volume.

The K(ψ) between soil layers was similar at matric potentials greater than −5 kPa, suggesting that the field capacity of the sandy soil was reached before −6 kPa [26]. The dependent relationship of unsaturated hydraulic conductivity K(θ) with the matric potential indicated that there are modifications in the soil water retention as a consequence of some variation in the pore distribution curve. Thus, the results of K(ψ) of the analyzed sandy soils

demonstrated that the evaluation of soil quality cannot be limited to the separation of TP into macroporosity and microporosity, but a detailed determination of the pore distribution curve is necessary [9].

4.1.3. Soil Water Retention

Higher soil water retention was observed in the subsurface layers (Table 2; Figure 2) due to the increase in microporosity, clay and silt contents, and reduction in coarse sand content at depth (Table 1). The relative error corresponded to 33.5% and 37.6% in the 0.2 to 0.4 m and 0.4 to 0.6 m layers relative to the subsurface layer, respectively. At potentials of −33 kPa, −100 kPa, and −500 kPa, the average relative errors were 35.6% and 39.5%. The largest relative errors (40.3% and 43.9%) occurred at the −1500 kPa matric potential.

Soil retains water due to capillary and adsorption matrix forces, which are responsible for water retention in the capillary pores of aggregates and on the surfaces of soil particles, respectively [49]. The surfaces of clays are negatively charged and adsorb a large number of water molecules on the soil surface due to their high specific surface area. For example, kaolinite can absorb 70,000 to 300,000 cm^2 of water/gram (g) per gram of kaolinite [3,50]. Thus, soil layers with higher clay contents retain more water in the soil, reinforcing the results obtained in this study.

The soils of the Caiuá Sandstone Formation have low clay content with a predominance of kaolinite (>80%), the presence of illite, a ratio of 2:1 clay to minerals, and small amounts of iron and aluminum oxides [16]. The Caiuá Sandstone Formation soils also have a high sand content, with a predominance of large pore diameters that are greater than 30 µm (Figure 3), which is drained at low matric potentials [9,51], reducing the water holding capacity of the soil.

The soil layer with higher fine sand content retained more soil water, especially at low matric potentials (less than −33 kPa; Figure 2). The obtained result reinforces the importance of the fractionation of total sand in sandy soils due to the higher specific surface area of fine sand at 318 cm^2/g compared to coarse sand at 79 cm^2/g [6,50]. The distribution between fine and coarse sand fractions is an inherent characteristic of soil formation and is not altered by management. Thus, it is worth emphasizing the importance that the accumulation of organic matter has in sandy soils because, besides increasing aggregation, it improves water retention and availability in soils [1,16,38,52,53].

Among the results obtained in the analyses of the soil water retention curves, it was verified that (1) the residual moisture (θr) was similar to the soil volumetric moisture at the hydraulic cut-off point (θ_{hco}) in the soil layers at depth ranges of 0 to 0.2 m (0.074 m^3/m^3), 0.2 to 0.4 m (0.120 m^3/m^3), and 0.4 to 0.6 m (0.126 m^3/m^3) (Table 2). Moreover, (2) the residual moisture (θr) was greater than the observed volumetric moisture at –1500 kPa. Finally, (3) the average relative difference in volumetric moisture at –500 and –1500 kPa was 12.92%, 6.03%, and 5.09% in the 0 to 0.2 m, 0.2 to 0.4 m, and 0.4 to 0.6 m layers, respectively. There are indications that the matric potential at the permanent wilting point occurs between −500 kPa and −1030 kPa at the hydraulic cut-off point.

Obtaining the true value of matric potential for improved agricultural crops has been a recurring discussion [54,55]. Torres et al., 2021 [55] found values for matric potential $\psi_{PMP} < -1500$ kPa and found that sunflower, corn, and soybean crops wilted at potentials lower than the estimated matric potentials in the hydraulic cut-off. When plants wilt at water suction lower than the hydraulic cut-off, the permanent wilting point is plant-limited, and when plants wilt at suctions greater than the hydraulic cut-off the limitation is from the soil [25].

Therefore, in sandy soils, obtaining the actual permanent wilting point should receive more attention. In the literature, in sandy texture soil (803 g/kg), there are indications that the average matric potential at the physiological permanent wilting point was –163.7 kPa (Mestre) and –241.7 kPa (Noble) for two modern wheat cultivars, and –90.9 kPa (ANAG 01) and –45.9 kPa (BRS Brau) for two barley cultivars [54].

The relative difference in volumetric moisture at –200 and –1030 kPa was 0.164%, 0.125% and 0.166% in soil layers 0 to 0.2 m, 0.2 to 0.4 m, and 0.4 to 0.6 m, respectively. However, it is critical to emphasize that no studies were found in the literature reporting the estimated matric potential at the physiological permanent wilting point for modern sugarcane cultivars from breeding programs. The hydraulic cut-off suction (–1030 kPa) lower than –1500 kPa reinforces the need for further studies for the sandy soil type analyzed.

Prevedello 1999 [26] found, in homogeneous and heterogeneous soil, that the drainage rate (τ) corresponded to p = 0.01 of the saturated soil hydraulic conductivity (τ = 0.01, K_S). Andrade and Stone 2011 [56] found matric potential at field capacity $\psi_{CC} = -6.5$ kPa, corresponding to $\hat{\theta}_{CC}$, for τ of 0.01 of K_S, in a sandy texture soil in the Cerrado. The moisture at the inflection point ($\hat{\theta}_{IP}$) is considered optimal for soil preparation [29] and correlates well with moisture at field capacity [56]. At the inflection point of the retention curve the first derivative changes from negative (convexity) to positive (concavity), and the second derivative is zero [57], which is relevant to determine the estimation of $\hat{\theta}_{CC}$.

An analysis of the moisture at the inflection point of the soil water retention curve (Table 5; Figure 2) indicated that the drainage rate of the soil corresponded to p = 0.050 of the K_S. The higher magnitude of the drainage rate of the analyzed soil was due to the texture, predominantly of the coarse sand fraction. For p = 0.050, there was ψ_{CC} of −4.602 kPa (0 to 0.2 m), −5.711 kPa (0.2 to 0.4 m), and −5.942 kPa (0.4 to 0.6 m). Regarding the time for field capacity to occur (t_{CC} measured in hours), the soil showed rapid vertical drainage due to the magnitude of the saturated hydraulic conductivity (K_S). In this case, the high magnitude of K_S influenced the low values of t_{CC}. The sand fraction of the soil also interferes with the matric potential corresponding to the permanent wilting point.

A higher magnitude of pore diameter was observed in the topsoil layer due to the higher coarse sand content (Table 1). The influence of the coarse sand fraction on the larger pore diameter and, consequently, lower water availability in predominantly sandy soils was also found by Fidalski et al., 2013 [6]. In soils with a predominance of sand, especially coarse sand, soil aggregation is reduced, not allowing the development of a more diverse pore network, especially in the smaller diameter pores, predominantly formed by organo-mineral interactions in the clay fraction [9,16]. Importantly, larger pore diameters require lower energy for soil water removal [9], consistent with results obtained for saturated hydraulic conductivity Ks and unsaturated hydraulic conductivity K(θ) (Figure 1).

4.1.4. Water Availability to Plants

Fidalski et al., 2013 [6] studied soils of the Paranavaí Sandstone Formation, in the northwestern region of Paraná and found that soil use and management interfered with water availability to plants. Fidalski et al., 2013 [6] also found available water capacity (AWC) in the layer between 0 and 0.4 m of 48.60 mm and 58.70 mm in soil under crop-livestock integration and pineapple, respectively. Helbel Junior and Fidalski 2017 [58] found an average water storage capacity of 1 mm/cm in the 0 to 0.6 m layer, in *Latossolo Vermelho distrófico* (Oxisol), medium texture, in the northwestern region of Paraná.

In the 0 to 0.6 m soil layer, the following were verified: AWC_1 = 68.78 mm; AWC_2 = 78.67 mm; EAW_1 = 64.03 mm and EAW_2 = 73.92 mm. AWC_2 overestimates soil water availability because the actual volumetric moisture at the permanent wilting point of the analyzed soil occurs before –1500 kPa (θ_{PMP}). EAW_1 underestimates soil water availability because the actual volumetric moisture at field capacity occurs at matric potentials lower than –6 kPa (θ_{CC}), highlighting the importance of the actual estimation of volumetric moisture at field capacity [56] and the hydraulic cut-off point [25].

Low water availability to plants in sandy soils can provide the occurrence of water deficit during the sugarcane cycle, as evidenced by Gurski et al., 2020 [59] and Araújo 2019 [60]. High soil hydraulic conductivity (K(θ)) and low time to reach moisture at field capacity (t_{CC}) intensify the occurrence of water deficit. Gurski et al., 2020 [59] verified that water deficiency and surplus were concentrated mainly in development phase II (vegetative growth), in the 1997-98 to 2008-09 crops, in Paranavaí, Paraná, requiring rescue irrigation.

Thus, the physical-hydric attributes determined in this study should be considered in the management of irrigation and the plant in each phase of its development.

The effect of sand contents on the water retention of the Caiuá Sandstone, from the northwestern Paraná region, was confirmed with the inverse correlation of coarse sand contents with microporosity, θ_{PMP}, clay, fine sand, and θ_{IP}, agreeing with [42]. The results again indicated the importance of a more detailed evaluation of the physical-hydric attributes of sandy soils, especially for monitoring the physical quality and water management in the analyzed soil.

4.2. Sustainability Implications

Soil type and properties at different depths influence the development of sugarcane [61]. While a shallow groundwater table can impact soil moisture dynamics [62], this research was conducted in an area that has a water table that is from 5 to 50 m deep [18], which is associated with vertical, subsurface soil water movement [17]. Yield modeling of sugarcane involves a detailed understanding of the impact of soil water storage dynamics on crop yield in Brazil. This is especially important for soils with low water holding capacity across water deficit gradients which have been modeled in northwestern São Paulo state using a crop water balance model combined with GIS [63]. In Köppen classification Cfa climates like in this study, the average yield response to full irrigation was 22 t/ha using the FAO-AZM simulation model [64]. Greater yield responses were in sandy soils with lower soil water holding capacities, where moisture from rainfall concentrated at the start of the dry season is not retained for as long as other soil types [64]. This research improves understanding of water dynamics for sugarcane grown in such sandy soils and how this relates to crop yield.

More accurate sugarcane models for Brazil's sandy soils are essential to optimize water management decisions to (1) invest in irrigation in order to increase crop productivity and to (2) withhold water, especially in irrigated systems prior to harvest to maximize sugar content. Yield gaps for sugarcane can be closed by using crop breeding for drought-tolerant cultivars [65] and irrigation [65,66]. If future climate changes increase sugarcane yield, payback for irrigation investments could decrease from 14 years to only 3 years, making such investments more feasible [67]. However, irrigation investments may be challenging since medium-sized sugarcane farms tend to be the most profitable [68], with potentially less capital available for such upfront purchases. Dias and Sentelhas 2018 [69] simulated sugarcane with APSIM-Sugar, showing stalk biomass reductions of 4% are ideal for maximizing sucrose yields. This can be accomplished by withholding water for drying off prior to harvest for 17 to 31 days for sandy soils with low water holding capacity [69].

The sustainable intensification of sugarcane, which includes increasing yield, has potential environmental benefits in addition to increased crop productivity. Sugarcane has been used recently to rehabilitate degraded pastures in Brazil. Luz et al., 2020 suggest that aside from compaction in the 10 to 20 cm soil layer, conversion from degraded pasture to sugarcane did not result in more soil degradation, whereas conversion from native habitat to extensive pasture resulted in severe soil degradation over time [70]. However, Dias et al., 2021 used APSIM-Sugar to show that climate change from RCP8.5 and RCP4.5 over the next century could result in sugarcane yield reductions in Brazil primarily due to water stress even with irrigation [64]. Future research is needed to improve the accuracy of sugarcane simulation models in sandy soils by validating models developed from experimental results from long-term sugarcane experiments with process-based sugarcane simulation models such as DSSAT-CANEGRO and APSIM-Sugar [71].

5. Conclusions

In this study, the main physical and hydric attributes of sandy soil were investigated for sugarcane cultivation in southern Brazil. Our results can guide future breeding programs to select sugarcane cultivars more tolerant to water deficit. In sandy soils with a total sand content close to 800 g/kg, the distribution of both coarse sand and fine sand fractions

should be measured to evaluate soil physical and hydric attributes, not just total sand content. The particle size of coarse sand ranges from 2 mm down to 0.2 mm while fine sand ranges from 0.2 to 0.05 mm. Higher coarse sand content increases saturated and unsaturated soil hydraulic conductivity, maximum pore diameter, and macroporosity, as well as reducing microporosity. A higher proportion of fine sand reduces conductivity and increases water retention, especially in deeper soil layers 0.4 to 0.6 m below the soil surface. The actual matric potential at field capacity was −4.60 kPa which is below the matric potential of −6 kPa commonly found in sandy soils in the topmost soil layer. The soil hydraulic cut-off point indicated that the matric potential of the permanent wilting point for sugarcane is reached at −1030 kPa, not −1500 kPa.

Although soil water retention increases with depth, its availability is greatest in the 0 to 0.2 m soil layer, with changes in the actual moisture at field capacity and permanent wilting point. The drainage rate of water at the soil surface is high. Therefore, there is a need for a continuous inflow of water into the soil, whether by precipitation or irrigation in order to ensure adequate soil moisture for the sugarcane crop. Sugarcane yield simulation using a locally validated model demonstrated that adequate crop yields are possible if there is adequate soil water storage for the sandy soils evaluated in this study. Future research can use actual moisture at field capacity and the permanent wilting point to develop a model for estimating sugarcane yield, considering the variation in soil water availability during the growth phase of sugarcane (phase II). This can be used to develop maps of soil water availability and yield estimates in the main sugarcane-producing regions for sandy soils.

Author Contributions: Conceptualization, J.L.V. and J.L.M.d.S.; methodology, J.L.V. and A.C.A.; software, J.L.V.; validation, J.L.V.; formal analysis, J.L.V.; investigation, J.L.V.; data curation, J.L.V.; writing—original draft preparation, J.L.V. and J.L.M.d.S.; writing—review and editing, J.L.V.; J.L.M.d.S., A.C.A., R.A.d.O., A.K.H., D.C.d.A., W.M.d.S. and R.M.A.; supervision, J.L.M.d.S.; project administration, R.A.d.O.; resources, A.K.H. All authors have read and agreed to the published version of the manuscript.

Funding: This research received funding support from Capes for the Doctoral Program of the lead author.

Institutional Review Board Statement: Not applicable.

Informed Consent Statement: Not applicable.

Data Availability Statement: Study data can be obtained by request to the corresponding author or the first author, via e-mail. It is not available on the website as the research project is still under development.

Acknowledgments: We would like to thank RIDESA for the availability of the experimental area and contribution to the research. We would also like to thank the Post-Graduate Program in Soil Science (UFPR), the Modeling of Agricultural Systems Laboratory (LAMOSA)/SCA/UFPR, and C. F. de Araújo-Júnior from the Rural Development Institute (IDR), Londrina, Paraná State. We are also grateful for the comments and edits from three anonymous reviewers which improved the quality of this work.

Conflicts of Interest: The authors declare no conflict of interest. Supporting entities had no role in the design of the study; in the collection, analyses, or interpretation of data; in the writing of the manuscript, or in the decision to publish the results.

References

1. Ferreira, M. Caracterização física do solo. In *Física do Solo*, 1st ed.; de Jong van Lier, Q., Ed.; Sociedade Brasileira de Ciência do Solo: Viçosa, Brasil, 2010; pp. 1–27.
2. Barbosa, L.C. Atributos Físicos do Solo e Desenvolvimento Radicular à Cana-Planta em Diferentes Sistemas De manejo. Master's Thesis, Universidade Estadual de Campinas, Faculdade de Engenharia Agrícola, Campinas, Brazil, 2015.
3. Silva, M.L.N.; Libardi, P.L.; Gimenes, F.H.S. Soil water retention curve as affected by sample height. *Rev. Bras. Ciênc. Solo* **2018**, *42*, 1–13. [CrossRef]

4. Stefanoski, D.C.; Santos, G.G.; Marchão, R.L.; Petter, F.A.; Pacheco, L.P. Uso e manejo do solo e seus impactos sobre a qualidade física. *Rev. Bras. Eng. Agríc. Ambient.* **2013**, *17*, 1301–1309. [CrossRef]
5. Souza, J.L.M.; Fezer, K.F.; Gurski, B.C.; Jerszurki, D.; Pachechenik, P.E.; Evangelista, A.W.P. Atributos físicos e balanço hídrico do solo com Floresta Ombrófila Mista, em Latossolo Vermelho-Amarelo, em Telêmaco Borba—PR. *Ciên. Florest.* **2018**, *28*, 90–101. [CrossRef]
6. Fidalski, J.; Tormena, C.A.; Alves, S.J.; Auler, P.A.M. Influência das frações de areia na retenção e disponibilidade de água em solos das Formações Caiuá e Paranavaí. *Rev. Bras. Ciên. Solo* **2013**, *37*, 613–621. [CrossRef]
7. Machado, J.L.; Tormena, C.A.; Fidalski, J.; Scapim, C.A. Inter-relações entre as propriedades físicas e os coeficientes da curva de retenção de água de um Latossolo sob diferentes sistemas de uso. *Rev. Bras. Ciênc. Solo* **2008**, *32*, 495–502. [CrossRef]
8. Cavalieri, K.M.V.; Carvalho, L.A.; Silva, A.P.; Libardi, P.L.; Tormena, C.A. Qualidade física de três solos sob colheita mecanizada de cana-de-açúcar. *Rev. Bras. Ciênc. Solo* **2011**, *35*, 1541–1549. [CrossRef]
9. Parahyba, R.B.V.; Araújo, M.S.B.; Almeida, B.G.; Rolim Neto, F.C.; Sampaio, E.V.S.B.; Caldas, A.M. Water retention capacity in Arenosols and Ferralsols in a semiarid area in the state of Bahia, Brazil. *An. Acad. Bras. Ciênc.* **2019**, *91*, 1–20. [CrossRef]
10. Daros, E.; Oliveria, R.A.; Zambon, J.L.C.; Bespalhok Filho, J.C.; Brasileiro, B.P.; Ido, O.T.; Ruaro, L.; Weber, H. RB036066—A sugarcane cultivar with high adaptability and yield stability to Brazilian South-Central region. *Crop Breed. Appl. Biotechnol.* **2018**, *18*, 325–329. [CrossRef]
11. Berton, G.S.; de Daros, O.R.A.E.; Zambon, J.L.C.; Bespalhok Filho, J.C.; Brasileiro, B.P.; Ido, O.T.; Ruaro, L.; Weber, H. RB036091—An early-maturing sugarcane cultivar for the Central South of Brazil. *Crop Breed. Appl. Biotechnol.* **2020**, *20*, 1–5. [CrossRef]
12. Santos, H.G.; Jacomine, P.K.T.; Anjos, L.H.C.; Oliveira, V.A.; Lumbreras, J.F.; Coelho, M.R.; Almeida, J.A.; Araújo Filho, J.C.; Oliverira, J.B.; Cunha, T.J.F. *Sistema Brasileiro de Classificação de Solos*, 5th ed.; Embrapa: Brasília, Brazil, 2018.
13. Nitsche, P.R.; Caramori, P.H.; Ricce, W.S.; Pinto, L.F.D. *Atlas Climático do Estado do Paraná*; Instituto de Desenvolvimento Rural do Paraná—IAPAR-EMATER: Londrina, Brazil, 2019.
14. FranchinI, J.C.; Veliini, C.L.; Balbinot Junior, A.A.; Debiasi, H.; Watanabe, R.H. *Integração Lavoura-Pecuária em Solo Arenoso e Clima Quente: Duas décadas de Experiência*; Circular Técnica 118; Embrapa Soja: Londrina, Brazil, 2016; pp. 1–11, ISSN 2176-2864. Available online: https://www.embrapa.br/en/busca-de-publicacoes/-/publicacao/1047856/integracao-lavoura-pecuaria-em-solo-arenoso-e-clima-quente-duas-decadas-de-experiencia (accessed on 24 April 2023).
15. MINOPAR—Minerais do Paraná S/A. Atlas geológico do Estado do Paraná. 2001. Available online: https://www.mineropar.gov.pr.br (accessed on 22 March 2023).
16. Costa, A.C.S.; Souza Junior, I.G.; Canton, L.C.; Gil, L.G.; Figueiredo, R. Contribution of the chemical and mineralogical properties of sandy-loam tropical soils to the cation exchange capacity. *Rev. Bras. Ciênc. Solo* **2020**, *44*, 1–18. [CrossRef]
17. Thomaz, E.L.; Fidalski, J. Interill erodibility of different sandy soils increases along a catena in the Caiuá Sandstone Formation. *Rev. Bras. Ciênc. Solo* **2020**, *44*, e0190064. [CrossRef]
18. Pereira, T.Y.Z. Avaliação da Vulnerabilidade e Fontes de Contaminações Difusas e Pontuais do Aquífero Caiuá. In *Monograph Course Conclusion Work (GC-119)*; Setor de Ciências da Terra, Curso de Geologia, Unversidade Federal do Paraná: Curitiba, Paraná, Brazil, 2016; pp. 1–32. Available online: https://www.geologia.ufpr.br/portal/wp-content/uploads/2018/10/Thomaz-Zulpo-TCC.pdf (accessed on 31 March 2023).
19. Empresa Brasileira de Pesquisa Agropecuária (EMBRAPA). *Manual de Métodos de Análise de Solo*, 2nd ed.; Embrapa Solos: Rio de Janeiro, Brazil, 2011; pp. 1–230.
20. Gubiani, P.I.; Reinert, D.J.; Reichert, J.M. Método alternativo para a determinação da densidade de partículas do solo—Exatidão, precisão e tempo de processamento. *Ciênc. Rural* **2006**, *36*, 664–668. [CrossRef]
21. Youngs, E.G. Hydraulic conductivity of saturated soils. In *Soil Analysis: Physical Methods*; Smith, K.A., Mullins, C.E., Eds.; Marcel Dekker: New York, NY, USA, 1991; Chapter 4; pp. 161–207.
22. Van Genuchten, M.T. A closed-form equation for predicting the hydraulic conductivity of unsaturated soils. *Soil Sci. Soc. Am. J.* **1980**, *44*, 892–898. [CrossRef]
23. Burdine, N.T. Relative permeability calculations from pore size distribution data. Petroleum Transactions. *Amer. Instit. Min. Metall. Eng.* **1953**, *198*, 71–78. [CrossRef]
24. R Core Team. *R: A Language and Environment for Statistical Computing*; R Foundation for Statistical Computing: Vienna, Austria, 2020; Available online: https://www.R-project.org/ (accessed on 3 January 2021).
25. Czyz, E.A.; Dexter, A.R. Influence of soil type on the wilting of plants. *Int. Agrophys.* **2013**, *27*, 385–390. [CrossRef]
26. Prevedello, C.L. Novo método para estimativa da umidade do solo na condição de capacidade de campo. *Rev. Bras. Recur. Hídr.* **1999**, *4*, 23–28. [CrossRef]
27. Sisson, J.B.; Fergusson, A.H.; van Genuchten, M.T. Simple method for predicting drainage from field plots. *Soil Sci. Soc. Am. J.* **1980**, *44*, 1147–1152. [CrossRef]
28. Prevedello, C.L.; Armindo, R.A. *Física do Solo com Problemas Resolvidos*, 2nd ed.; Celso Luiz Prevedello: Curitiba, Brazil, 2015; pp. 1–474, ISBN 978-8590757429.
29. Dexter, A.R.; Bird, N.R.A. Methods for predicting the optimum and the range of soil water contents for tillage based on the water retention curve. *Soil Tillage Res.* **2001**, *57*, 203–212. [CrossRef]
30. Libardi, P.L. *Dinâmica da Água no Sol*, 2nd ed.; Editora da Universidade de São Paulo: São Paulo, Brazil, 2012; ISBN 978-8531417054.
31. Willmott, C.J. Some comments on the evaluation of model performance. *Bull. Am. Meteorol. Soc.* **1982**, *63*, 1309–1313. [CrossRef]

32. Mangiafico, S.S. Summary and Analysis of Extension Program Evaluation in R, Version 1.18.1. 2016. Available online: https://rcompanion.org/handbook (accessed on 10 January 2021).
33. Horikoshi, M.; Tang, Y. ggfortify: Data Visualization Tools for Statistical Analysis Results. 2016. Available online: https://CRAN.R-project.org/package=ggfortify (accessed on 28 January 2021).
34. Viana, J.L.; de Souza, J.L.M.; Hoshide, A.K.; de Oliveira, R.A.; de Abreu, D.C.; da Silva, W.M. Estimating Sugarcane Yield in a Subtropical Climate Using Climatic Variables and Soil Water Storage. *Sustainability* **2023**, *15*, 4360. [CrossRef]
35. Parahyba, R.B.V.; Almeida, B.G.; Rolim Neto, F.C.; Araújo, M.S.B. Condutividade hidráulica dos solos arenosos da região semiárida da Bacia sedimentar do Tucano no município de Glória, Bahia, Brasil. In Proceedings of the III Reunião Nordestina de Ciência do Solo: Integração e Uso do Conhecimento para Uma Agricultura Sustentável no Nordeste, Aracajú, Brazil, 12–15 September 2016; Available online: https://www.embrapa.br/en/busca-de-publicacoes/-/publicacao/1058873/condutividade-hidraulica-dos-solos-arenosos-da-regiao-semiarida-da-bacia-sedimentar-do-tucano-no-municipio-de-gloria-bahia-brasil (accessed on 24 April 2023).
36. Moriasi, D.N.; Arnold, J.G.; van Liew, M.W.; Bingner, R.L.; Harmel, R.D.; Veith, T.L. Model evaluation guidelines for systematic quantification of accuracy in watershed simulations. *Trans. ASABE* **2007**, *50*, 885–900. [CrossRef]
37. Souza, J.L.M.; Gerstemberger, E.; Gurski, B.C.; Oliveira, R.A. Adjustment of water-crop production models for ratoon sugarcane. *Pesqui. Agropecu. Trop.* **2015**, *45*, 426–433. [CrossRef]
38. Rawls, W.J.; Pachepsky, Y.A.; Ritchie, J.C.; Sobecki, T.M.; Bloodworth, H. Effect of soil organic carbon on soil water retention. *Geoderma* **2003**, *116*, 61–76. [CrossRef]
39. Soil Science Division Staff. *Soil Survey Manual, USDA Handbook 18*; Ditzler, C., Scheffe, K., Monger, H.C., Eds.; Government Printing Office: Washington, DC, USA, 2017; pp. 1–603.
40. Fracaro, F.; Lamb, C.R.C.; Straaburge, A.S.; Lattuada, D.S.; Buttow, M.V.; Monttero, C.R.S.; Silva, S.D.A. Avaliação agronômica de genótipos de cana-de-açúcar em Via-mão/RS. In *Simpósio Estadual de Aroenergia; Reunião Técnica de Agroenergia—RS, 5*; Encontro de Energias Renováveis na Agricultura Familiar, 2. Pelotas; Embrapa Clima Temperado: Pelotas, Brazil, 2014; pp. 1–4. Available online: https://www.embrapa.br/en/busca-de-publicacoes/-/publicacao/1005818/avaliacao-agronomica-de-genotipos-de-cana-de-acucar-em-viamaors (accessed on 4 April 2023).
41. CONAB (Companhia Nacional de Abastecimento). Acompanhamento da Safra Bra-Sileira de Cana-de-Açúcar, Safra 2022/23–Terceiro Levantamento, Brasília, Distrito Federal, Brazil. Available online: https://www.conab.gov.br/info-agro/safras/cana (accessed on 4 April 2023).
42. Fidalski, J. Disponibilidade de água e comportamento físico dos solos da Formação Arenito Caiuá. In *V Reunião Paranaense de Ciência do Solo e II Simpósio Brasileiro de Solos Arenosos*; Maringá, Livro Eletrônico; SBCS/NEPAR: Curitiba, Brazil; IAPAR: Londrina, Brazil, 2017.
43. Ortiz, P.F.S.; Rolim, M.M.; Lima, J.L.P.; Pedrosa, E.M.R.; Dantas, M.S.M.; Tavares, U.E. Physical qualities of an Ultisol under sugarcane and Atlantic forest in Brazil. *Geoderma Reg.* **2017**, *11*, 62–70. [CrossRef]
44. Cabral, M.C.M.; Carvalho, L.A.; Novak, E.; Schicarelli, C.D.S. Sistema de preparo de solo em área de reforma de canavial e as alterações físicas do solo. *Rev. Agrar.* **2015**, *8*, 376–386.
45. Arcoverde, S.N.S.; Souza, C.M.A.; Suarez, A.H.T.; Colman, B.A.; Nagahama, H.J. Atributos físicos do solo cultivado com cana-de-açúcar em função do preparo e época de amostragem. *Rev. Agric. Neotrop.* **2019**, *6*, 41–47. [CrossRef]
46. Jadczyszyn, J.; Niedzwiecki, J. Relation of Saturated Hydraulic Conductivity to Soil Losses. *Pol. J. Environ. Stud.* **2005**, *14*, 431–435.
47. Cherubin, M.R.; Karlen, D.L.; Franco, A.L.; Tormena, C.A.; Cerri, C.E.; Davies, C.A.; Cerri, C.C. Soil physical quality response to sugarcane expansion in Brazil. *Geoderma* **2016**, *267*, 156–168. [CrossRef]
48. Silva, P.L.F.; Oliveira, F.P.; Borba, J.O.M.; Tavares, D.D.; do Amaral, A.J.; Martins, A.F. Solos arenosos para Sistemas de integração lavoura-pecuária-floresta em Arez, Rio Grande do Norte. Rev. *Verde de Agroecol. Desenvolv. Sust.* **2018**, *13*, 581–589. [CrossRef]
49. Libardi, P.L. Água no solo. In *Física do Solo*, 1st ed.; de Jong van Lier, Q., Ed.; Sociedade Brasileira de Ciência do Solo: Viçosa, Brazil, 2010; pp. 101–152.
50. Giasson, E. Introdução ao estudo dos solos. In *Fundamentos de Química do Solo*, 6th ed.; Meurer, E.J., Ed.; Evangraf Publishing, Ltd.: Porto Alegre, Brazil, 2017; pp. 11–28.
51. Costa, A.; Albuquerque, J.A.; Costa, A.; Pértile, P.; Silva, F.R. Water retention and availability in soils of the state of Santa Catarina-Brazil: Effect of textural classes, soil classes and lithology. *Rev. Bras. Ciênc. Solo* **2013**, *37*, 1535–1548. [CrossRef]
52. Lopes, I.M.; Ziviani, M.M.; Pinto, L.A.S.; Pinheiro, E.F.M.; Weber, H.; Pereira, M.G.; Lima, E.; Campos, D.V.B. Agregação e distribuição do carbono nos agregados de Latossolo Vermelho sob diferentes níveis de palhada da cana-de-açúcar em Paranavaí (PR). *Rev. Virtual Quím.* **2017**, *9*, 1985–1995. [CrossRef]
53. Auler, A.C.; Romaniw, J.; Sá, J.C.M.; Pires, L.F.; Hartman, D.C.; Inagaki, T.M.; Rosa, J.A. Improvement on soil structure and water retention after application of industrial organic waste as a crop fertilizer. *J. Soils Sedim.* **2020**, *20*, 2771–2783. [CrossRef]
54. Wiecheteck, L.H.; Giarola, N.F.B.; Lima, R.P.; Tormena, C.A.; Torres, L.C.; Paula, A.L. Comparing the classical permanent wilting point concept of soil (−15,000 hPa) to biological wilting of wheat and barley plants under contrasting soil textures. *Agric. Water Manag.* **2020**, *230*, 105965. [CrossRef]
55. Torres, L.C.; Keller, T.; Lima, R.P.; Tormena, C.A.; Lima, H.V.; Giarola, N.F.B. Impacts of soil type and crop species on permanent wilting of plants. *Geoderma* **2020**, *384*, 114798. [CrossRef]

56. Andrade, R.S.; Stone, L.F. Estimativa da umidade na capacidade de campo em solos sob Cerrado. *Rev. Bras. Eng. Agríc. Ambient.* **2021**, *15*, 111–116. [CrossRef]
57. Silva, A.P.; Tormena, C.A.; de Dias Júnior, M.S.; Imhoff, S.; Klein, V.A. Indicadores da qualidade física do solo. In *Física do Solo*, 1st ed.; de Jong van Lier, Q., Ed.; Sociedade Brasileira de Ciência do Solo: Viçosa, Brazil, 2010; pp. 241–281.
58. Helbel Junior, C.; Fidalski, J. Parâmetros técnicos sobre o armazenamento de água no solo na Região Noroeste do Paraná. In *V Reunião Paranaense de Ciência do Solo e II Simpósio Brasileiro de Solos Arenosos. Livro Eletrônico*; SBCS/NEPAR: Curitiba, Brazil; IAPAR: Londrina, Brazil, 2017.
59. Gurski, B.C.; Souza, J.L.M.; Gerstemberg, E.; Oliveira, R.A. Water requirements and restrictions to sugarcane in cane plants and ratoon cane cycles in Southern Brazil. *Acta Agron.* **2020**, *69*, 136–144. [CrossRef]
60. Araújo, R.M. Influência das Condições Climáticas no Crescimento e Desenvolvimento da Cana-de-Açúcar na Região sul do Brasil. Ph.D. Thesis, Programa de Pós-Graduação em Agronomia (Produção Vegetal), Setor de Ciências Agrárias, Universidade Federal do Paraná, Curitiba, Brazil, 2019.
61. Amorim, M.T.A.; Silverio, N.E.Q.; Bellinaso, H.; Gómez, A.M.R.; Greschuk, L.T.; Campos, L.R.; Demattê, J.A.M. Impact of soil types on sugarcane development monitored over time by remote sensing. *Precis. Agric.* **2022**, *23*, 1532–1552. [CrossRef]
62. Liu, Z.L.; Wang, C.; Zhang, L.; Wang, X.; Huang, G.; Xu, X.; Steenhuis, T.S. A field-validated surrogate crop model for predicting root-zone moisture and salt content in regions with shallow groundwater. *Hydrol. Earth Syst. Sci.* **2020**, *24*, 4213–4237. [CrossRef]
63. Perin, V.; Sentelhas, P.C.; Dias, H.B.; Santos, E.A. Sugarcane irrigation potential in Northwestern São Paulo, Brazil, by integrating Agrometeorological and GIS tools. *Agric. Water Manag.* **2019**, *220*, 50–58. [CrossRef]
64. Dias, H.B.; Sentelhas, P.C.; Inman-Bamber, G.; Everingham, Y. Sugarcane yield future scenarios in Brazil as projected by the APSIM-Sugar model. *Ind. Crops Prod.* **2021**, *171*, 113918. [CrossRef]
65. Xu, C.; Mao, J.; Li, X.; Burner, D.M.; Li, C.; Hussin, S.H.H.; Lin, X.; Liu, H.; Zhao, P.; Lu, X.; et al. Evaluating of drought tolerance in sugarcane genotypes using the membership function value of drought tolerance (MFVD). *Euphytica* **2023**, *219*, 37. [CrossRef]
66. Dias, H.B.; Sentelhas, P.C. Sugarcane yield gap analysis in Brazil—A multi-model approach for determining magnitudes and causes. *Sci. Total Environ.* **2018**, *637–638*, 1127–1136. [CrossRef] [PubMed]
67. de Castro Mattos, E.; Tomé, T.C.H.; Menillo, R.B.; Marin, F.R. Simulating of Future Climate Conditions on the Effect of Irrigation on Sugarcane Yield in Southern Brazil. *Braz. J. Agric.* **2021**, *96*, 446–470. [CrossRef]
68. Patino, M.T.O.; de Amorim, F.R.; de Andrade, A.G.; Alam, M.J.; Solfa, F.D.G. Costs of Agronomic Practices: Profitability at Different Scales of Sugarcane Production in Brazil. *Int. J. Bus. Adm.* **2022**, *13*, 32–43. [CrossRef]
69. Dias, H.B.; Sentelhas, P.C. Drying-off Periods for Irrigated Sugarcane to Maximize Sucrose Yields under Brazilian Conditions. *Irrig. Drain.* **2018**, *67*, 527–537. [CrossRef]
70. da Luz, F.B.; Carvalho, M.L.; de Borba, D.A.; Schiebelbein, B.E.; de Lima, R.P.; Cherubin, M.R. Linking Soil Water Changes to Soil Physical Quality in Sugarcane Expansion Areas in Brazil. *Water* **2020**, *12*, 3156. [CrossRef]
71. Dias, H.B.; Inman-Bamber, G. Sugarcane: Contribution of Process-Based Models for Understanding and Mitigating Impacts of Climate Variability and Change on Production. In *Systems Modeling*; Springer Nature: Singapore, 2020; Chapter 8; pp. 217–260. [CrossRef]